


 Cite this: *RSC Adv.*, 2022, **12**, 7830

 Received 10th January 2022  
 Accepted 25th February 2022

DOI: 10.1039/d2ra00176d

[rsc.li/rsc-advances](http://rsc.li/rsc-advances)

## Dispersing carbomers, mixing technology matters!<sup>†</sup>

 Maarten Houleberghs,<sup>a</sup> Loes Verheyden,<sup>a</sup> Filip Voorspoels,<sup>c</sup>  
 C. Vinod Chandran,<sup>ab</sup> Karel Duerinckx,<sup>ab</sup> Sambhu Radhakrishnan,<sup>ab</sup>  
 Johan A. Martens<sup>ab</sup> and Eric Breynaert<sup>\*ab</sup>

Mixing dry carbomer powder with water using magneto-hydrodynamic mixing yielded carbomer dispersions with higher viscosity and increased storage modulus as compared to conventional high shear mixing. <sup>1</sup>H NMR spectroscopy demonstrated this to be induced by a different water distribution, accompanied by lower ionization and higher degradation of the polymer in case of high shear mixing. This investigation reveals <sup>1</sup>H MAS NMR to provide suitable sensitivity and resolution to detect structural changes induced in organic polymers during their hydration.

Polymer based hydrogels are widely applied in the cosmetic, pharmaceutical, paint, and food industries. Their tunable viscosity, unique visco-elastic properties and low toxicity renders them very attractive as thickening, suspending, dispersing, and stabilizing agents.<sup>1–3</sup> Carbomer hydrogels, in particular, have been in high demand since the start of the COVID-19 pandemic as they are often used for preparing hand sanitizing hydro-alcoholic gels. Carbomer hydrogels are typically prepared by hydration and neutralization of high molecular weight, cross-linked polyacrylic acids, typically using energy-intensive high shear mixers to accelerate the hydration process.<sup>4–9</sup> High shear mixers exploit the rotor–stator principle to generate shear forces and turbulence within a fluid, thus enabling mixing. Important drawbacks of this technology are its high-energy demand and the generation of heat as a result of friction near the rotor. The latter can lead to thermal degradation of thermolabile compounds, especially for long mixing times within viscous mixtures, as the viscosity hinders heat dissipation.<sup>7,10</sup> In the case of carbomer hydrogels, shear can damage the hydrated polymer chains, resulting in a permanent loss of viscosity, in some cases as high as 50%.<sup>9,10</sup> In spite of these shortcomings, high shear mixers (HSM) continue to be the industrial standard for production of carbomer hydrogel from the powdered polymer for lack of a better alternative.<sup>6–9</sup>

This work explores a radical new approach for mixing and preparing highly stable, high viscosity carbomer dispersions. Magneto-hydrodynamic (MHD) mixing is a mixing principle

based on the application of a magnetic field on a fluid stream flowing in a turbulent flow regime.<sup>11</sup> While it has been shown that the combination of turbulent flow with a permanent magnetic field induces complex effects, including efficient mixing, de-agglomeration of clustered particles or creation of long-lived states,<sup>12–16</sup> there is no comprehensive scientific description of the phenomena. Turbulent flow mixing is characterized by an irregular mixing pattern in randomly moving eddies, rendering the evaluation of the impact of a permanent magnetic field on a colloidal system in a turbulent flow condition very complex. Experimental observations reveal that the magnetic field is responsible for additional shear, electrostatic, tensile and oscillatory forces.

To evaluate its performance, carbomer hydrogels containing 1.22 wt% Carbopol® were prepared using either magneto-hydrodynamic mixing or conventional high shear mixing. The carbomer dispersions were characterized using rheology and <sup>1</sup>H MAS NMR spectroscopy. Experiments were performed with Carbopol® 980 NF (Lubrizon),<sup>17</sup> a synthetic homopolymer of polyacrylic acid (PAA) cross-linked with allyl pentaerythritol. Carbopol® 980 NF is available as a dry powder with a primary particle size averaging around 0.2 μm in diameter. Each particle is composed of tightly coiled linear polymer chains, soluble in polar liquids such as water.<sup>1,17</sup> Upon initial mixing with water, the polymer forms an acidic dispersion (pH ≈ 3) of tightly wound polymer chains that start to unfold following hydration and deprotonation of the carboxylic acid groups (Fig. 1). The presence of these carboxyl moieties also renders polyacrylic acid responsive to changes in pH and ionic strength. Following initial hydration, neutralization of the aqueous PAA dispersion with a base typically yields a gel matrix exhibiting increased viscosity with increasing pH (up to a pH of 10). Deprotonation of the carboxyl moieties generates localised negative charges on the polymer (Fig. 1), promoting unfolding and enhancing viscosity by electrostatic repulsion.<sup>18–22</sup> This work reveals <sup>1</sup>H

<sup>a</sup>Characterization and Application Team (COK-kat), KU Leuven, 3001 Heverlee, Belgium. E-mail: [eric.breynaert@kuleuven.be](mailto:eric.breynaert@kuleuven.be)

<sup>b</sup>NMR-Xray platform for Convergence Research (NMRCoRe), KU Leuven, 3001 Heverlee, Belgium

<sup>c</sup>Master of Bioscience Engineering: Catalytic Technology, KU Leuven, Belgium

<sup>†</sup> Electronic supplementary information (ESI) available: Technical specifications mixing setups, experimental procedures, measurement protocols, theoretical <sup>1</sup>H chemical exchange models, temperature profiles. See DOI: 10.1039/d2ra00176d



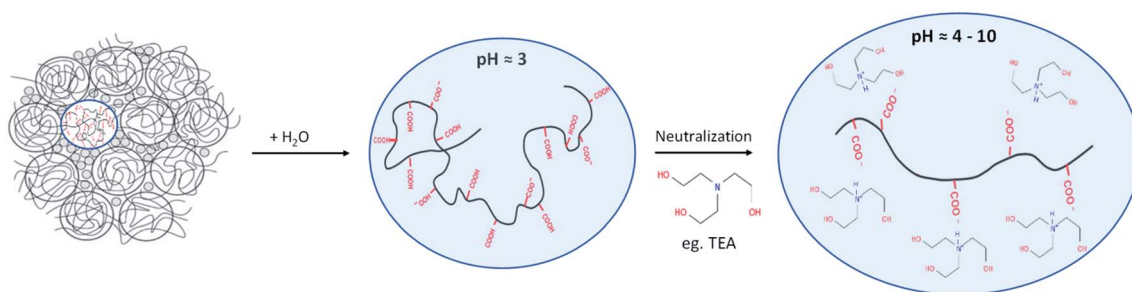


Fig. 1 Schematic representation of carbomer polymer folding in different conditions. Hydration of the polymer leads to unfolding of the tightly coiled chains. Deprotonation of the carboxylic acid functional groups results in the development of a pH dependent negative charge. With increasing pH, increased intra-molecular electrostatic repulsion amplifies polymer chain unfolding, yielding a viscous hydrogel. Adapted from Shafiei *et al.* (2018).<sup>6</sup>

MAS NMR to provide suitable sensitivity and resolution to detect structural changes induced in organic polymers during their hydration. Magneto-hydrodynamic mixing was shown to not only induce less structural damage during the mixing process, as compared to high shear mixing, magneto-hydrodynamic mixing also generates long-lived charge stabilization on the polymer, giving rise to enhanced properties of the hydrated carbomer dispersion.

Fig. S1 and S2 (ESI<sup>†</sup>) show schematic representations of, respectively, the high shear mixer (HSM) and the magneto-hydrodynamic (MHD) mixing setup used in this study. The absence of rotating components in the latter setup allows the MHD mixing setup to be powered by a 1.5 kW screw pump, whereas the HSM setup requires an 11 kW mixer. In both setups, a temperature probe is positioned inside the tank to monitor the temperature evolution of the mixture (Fig. S3, ESI<sup>†</sup>). Technical and procedural details are provided in the Process description section of the ESI.<sup>†</sup> In all experiments, a carbomer dispersion with nominal carbomer concentration of 1.22 wt% was produced by mixing 435.84 g Carbopol<sup>®</sup> 980 NF powder with 35.28 L of demineralized water using either the high-shear or the magneto-hydrodynamic mixing technology. In every experiment, the polymer dispersion was sampled after 1 and 3 minutes of mixing. Independent of the mixing technology used, after 1 minute of mixing the carbomer dispersion exhibited a pH of 2.7. Longer mixing times did not significantly change the pH of the dispersion. Despite the similarity in pH observed after 3 minutes of mixing, rheological characterization of the samples revealed a consistently higher viscosity for the sample mixed with MHD equipment compared to HSM (Fig. 2, left).

Next to a method-of-mixing dependent viscosity, the samples also exhibit method-of-mixing dependent storage moduli ( $G'$ ).  $G'$  represents the energy stored in the material upon deformation. This is known to increase with increasing crosslinking inside the polymer particles. As shown in Fig. 2 (right),  $G'$  is consistently higher for the MHD – 3 min sample compared to HSM – 3 min.

Molecular level information explaining the method-of-mixing dependent visco-elastic properties of the Carbopol<sup>®</sup> hydrogels was obtained using <sup>1</sup>H nuclear magnetic resonance

(NMR) spectroscopy. Comparing the water region of direct excitation <sup>1</sup>H MAS NMR spectra collected on carbomer dispersions obtained after 1 and 3 minutes of high shear or magneto-hydrodynamic mixing, a difference in the water populations is readily observed (Fig. 3a). After 1 minute of high shear mixing, the aqueous carbomer solution exhibits two distinct envelopes of <sup>1</sup>H resonances (Fig. 3a, HSM – 1), while the MHD technology gives rise to a single water envelope with maximum at 4.84 ppm. The signals with maxima around 4.85 and 4.83 ppm were tentatively assigned to bulk-like water (in between partially hydrated carbomer particles) and to water hydrating the carbomer backbone, respectively. This assignment can be rationalized by considering the mixing procedure. Mixing dry carbomer powder into a liquid water phase initially generates an aqueous suspension of partially hydrated particles in which most polymer chains are still tightly entangled. Whereas MHD technology seem to nearly instantly induce a homogeneous hydration of the polymer, the high shear mixing process clearly creates isolated pockets of water which are literally 'beaten' into the dense carbomer phase through high shear forces. Water molecules in the solvent behave like bulk water, while water molecules hydrating the bundles of polymer reside in a highly organic local environment, resulting in a lower <sup>1</sup>H chemical shift. The lower chemical shift is similar to what is observed for water contained in nanoscopic water clusters dispersed in hydrophobic solvents.<sup>23,27</sup>

The molecular picture sketched above is derived from <sup>1</sup>H-<sup>1</sup>H exchange spectroscopy (EXSY) (Fig. 3c and d). As seen in Fig. 3c, the HSM sample obtained after 1 minute contains two physically separated water pools exhibiting only very limited chemical exchange between the pools. With increasing mixing time, the two envelopes of <sup>1</sup>H resonances merge together into a single envelope. As indicated by the EXSY spectrum of the HSM sample obtained after 3 minutes (Fig. 3d), the merge is the result of chemical exchange. With increasing mixing time, the polymer increasingly unfolds yielding a fully hydrated polymer phase homogeneously dispersed in water and allowing for proton exchange between the solvent water and the water hydrating the polymer. As experimentally demonstrated by the EXSY spectrum in Fig. 3d and as shown in Fig. S4 (ESI<sup>†</sup>) using a theoretical exchange model, the single envelope of water-



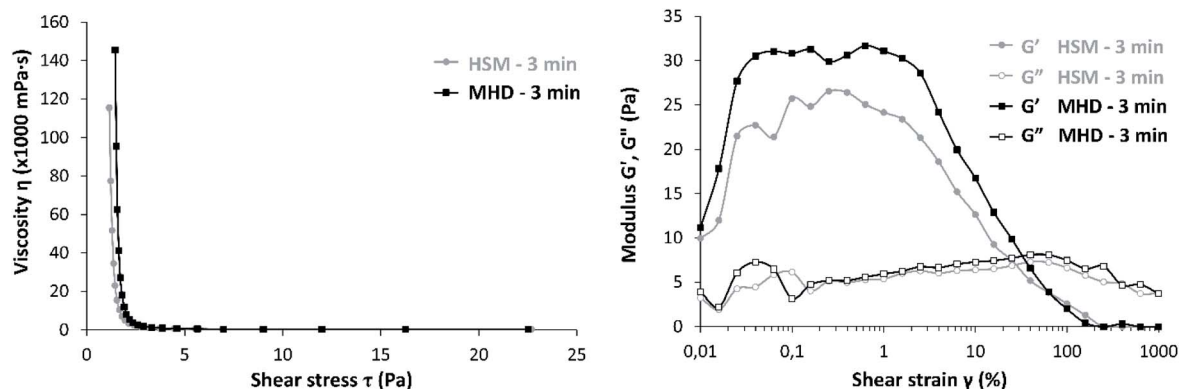


Fig. 2 Left: viscosity measurement as function of applied shear stress for aqueous carbomer dispersions (1.22 wt% Carbopol®) mixed for 3 minutes with HSM and MHD. Right: strain sweep test results, plotted as storage ( $G'$ ) and loss ( $G''$ ) modulus vs. applied shear strain ( $\gamma$ ).

derived  $^1\text{H}$  resonances centered around 4.84 ppm results from chemical exchange between multiple water populations occurring in the range between 4.85 and 4.83 ppm. In the case of the MHD mixing technology, the water distribution centered around 4.84 ppm was already achieved after 1 minute, hinting

at a superior mixing and hydrating efficiency of the carbomer powder compared to the HSM technology (Fig. 3a, MHD – 1 min).

Next to the water region in the  $^1\text{H}$  MAS NMR spectra, also the  $\text{CH}_3$ ,  $\text{CH}_2$  and  $\text{CH}$  region reveals important information on the

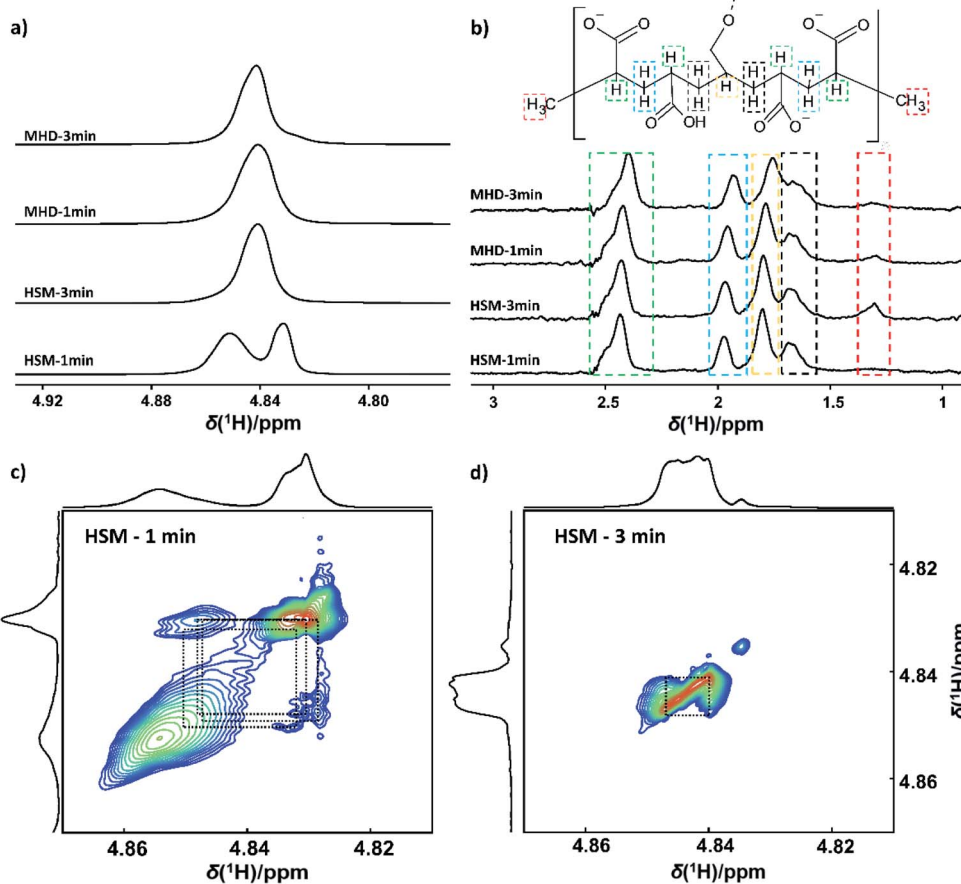


Fig. 3 (a)  $^1\text{H}$  NMR spectra of the different carbomer gels prepared under HSM and MHD mixing conditions using different mixing times. (b) Enlarged view of the  $^1\text{H}$  NMR spectra between 1 and 3 ppm, highlighting the  $^1\text{H}$  resonances originating from the PAA backbone of the carbomer. The different  $^1\text{H}$  signals have been assigned using color coding. (c)  $^1\text{H}$ - $^1\text{H}$  exchange spectroscopy (EXSY) spectra of the carbomer gel prepared with HSM after 1 minute and (d) after 3 minutes of mixing.



molecular state of the carbomer polymer in the dispersions. Detailed inspection of the  $^1\text{H}$  NMR spectra reveals increasing shift of the resonances associated with the protons of the polyacrylic acid backbone with increasing mixing time (Fig. 3b). This downward shift not only increases with mixing time, it is also higher for the sample series prepared using MHD technology as compared to dispersions prepared using the HSM technology (Fig. 3b). The occurrence of this downward shift is an indication that different mixing technologies as well as increased mixing times introduce differences in the local charge distribution on the polymer. The  $^1\text{H}$  NMR resonances of  $\alpha$ - and  $\beta$ -protons of carboxylic acids have been shown to shift to lower chemical shifts with increasing local chemical charge on the polymer and, hence, with increasing deprotonation of the carboxylic moieties.<sup>24,25</sup> This molecular level observation is consistent with the macroscopic observations from rheological characterization. MHD technology produces more viscous hydrogels with an increased shelf life, all other sample production parameters being identical. This is most likely the result of an increased unfolding of the polymer chains in combination with an enhanced charge stabilization of the polymer dispersion. The shelf life of the hydrogels was evaluated by measuring the decrease in viscosity over time. Dispersions prepared with MHD technology proved more stable, with an average viscosity loss of 126 mPa s per day compared to 223 mPa s in the case of high shear mixing. In both cases, the decrease in viscosity was associated with demixing of the aqueous phase most likely due to the influence of gravity (Fig. S5, ESI<sup>†</sup>).

The direct excitation  $^1\text{H}$  MAS NMR spectra shown in Fig. 3b were recorded quantitatively, ensuring an identical filling factor of the coil and similar  $Q$ -factor of the probe head RF circuit.<sup>26</sup> This enables comparison of the area of the methyl resonances, readily revealing an increase in the concentration of terminal methyl groups (1.3 ppm) when using HSM compared to MHD mixing technology. With increased mixing time, the area of the resonance at 1.3 ppm almost tripled when using HSM, while it remained constant for extended mixing times in the MHD mixer (Table S1, ESI<sup>†</sup>). These additional terminal methyl groups are produced during the mixing process, most likely as result of cleavage of longer polymer chains upon exposure to high shear forces. This mechanical degradation reduces the overall degree of crosslinking within the polymer, and can help explain the negative impact of high shear mixing on the viscosity and the storage modulus  $G'$  of the carbomer samples.

In summary, it was shown that magneto-hydrodynamic (MHD) mixing can be an alternative to conventional high shear mixing (HSM) for preparing highly stable carbomer dispersions. Compared to high shear mixing, magneto-hydrodynamic mixing enables the production of high viscosity dispersions using lower polymer concentrations and using shorter mixing times while in addition requiring less energy (1.5 kW for the MHD mixing setup vs. 11 kW for the high shear mixer). The present study also showed that the dependence of the rheological properties of carbomer dispersions on mixing time and mixing technology has a molecular level origin. Comparing samples prepared using high-shear *versus*

magneto-hydrodynamic mixing technologies,  $^1\text{H}$  NMR spectroscopy demonstrated the macroscopic rheological effects to be due to the occurrence of different water distributions and a lower ionization and higher degree of degradation of the carbomer polymers in case of high shear mixing. Preparing carbomer dispersions with a carbomer content of 1.22 wt%, hydration of the carbomer using MHD technology proved to be more time efficient. After a same time of mixing, MHD technology enables to produce aqueous carbomer dispersions with higher viscosity and higher storage modulus  $G'$  as compared to high shear mixing.  $^1\text{H}$  MAS NMR was shown to be an ideal method to reveal the degree of structural damage induced during mixing and to detect the occurrence of long-lived states contributing to the stability of the hydrated polymer dispersion by stabilizing charge on the polymer.

## Conflicts of interest

The authors declare no conflict of interest.

## Acknowledgements

This work was supported by the ERC through an Advanced Research Grant under the European Union's Horizon 2020 research and innovation programme (No. 834134 WATUSO). NMRCoRe acknowledges the Flemish government, department EWI for financial support as International Research Infrastructure (I001321N: Nuclear Magnetic Resonance Spectroscopy Platform for Molecular Water Research). J. A. M. acknowledges the Flemish Government for long-term structural funding (Methusalem) and department EWI for infrastructure investment *via* the Hermes Fund (AH.2016.134). M. H. and E. B. also acknowledge FWO for an FWO-SB fellowship and a research grant (1.5.061.18N), respectively.

## Notes and references

- 1 P. R. Varges, C. M. Costa, B. S. Fonseca, M. F. Naccache and P. R. De Souza Mendes, *Fluids*, 2019, **4**, 3–22.
- 2 P. Panzade and P. K. Puranik, *Res. J. Pharm. Technol.*, 2010, **3**, 672–675.
- 3 S. A. Varghese, S. M. Rangappa, S. Siengchin and J. Parameswaranpillai, in *Hydrogels Based on Natural Polymers*, ed. Y. Chen, Elsevier, 2020, pp. 17–47.
- 4 Silverson, Dispersion and Hydration of Carbopol®, <https://www.silverson.com/us/resource-library/application-reports/dispersion-and-hydration-of-carbopol>, accessed 1 June 2021.
- 5 Admix, Carbopol® Mixing/Carbomer Processing Equipment, <https://www.admix.com/carbopol>, accessed 28 May 2021.
- 6 M. Shafiei, M. Balhoff and N. W. Hayman, *Polymer*, 2018, **139**, 44–51.
- 7 J. Zhang, S. Xu and W. Li, *Chem. Eng. Process.*, 2012, **57–58**, 25–41.
- 8 M. Dinkgreve, M. Fazilati, M. M. Denn and D. Bonn, *J. Rheol.*, 2018, **62**, 773–780.
- 9 L. Baudonnet, D. Pere, P. Michaud, J. L. Grossiord and F. Rodriguez, *J. Dispersion Sci. Technol.*, 2002, **23**, 499–510.



- 10 The Lubrizol Corporation, TDS-103 Dispersion Techniques for Carbopol® Polymers, [https://www.lubrizol.com/-/media/Lubrizol/Health/TDS/TDS-103\\_Dispersion\\_Techniques\\_Carbopol\\_Polymers.pdf](https://www.lubrizol.com/-/media/Lubrizol/Health/TDS/TDS-103_Dispersion_Techniques_Carbopol_Polymers.pdf), accessed 1 June 2021.
- 11 S. Kerkhofs, H. Lipkens, F. Velghe, P. Verlooy and J. A. Martens, *J. Food Eng.*, 2011, **106**, 35–39.
- 12 E. Breynaert, J. Emmerich, D. Mustafa, S. R. Bajpe, T. Altantzis, K. Van Havenbergh, F. Taulelle, S. Bals, G. Van Tendeloo, C. E. A. Kirschhock and J. A. Martens, *Adv. Mater.*, 2014, **26**, 5173–5178.
- 13 B. Stuyven, J. Emmerich, P. Eloy, J. Van Humbeeck, C. E. A. Kirschhock, P. A. Jacobs, J. A. Martens and E. Breynaert, *Appl. Catal., A*, 2014, **474**, 18–25.
- 14 B. Stuyven, Q. Chen, W. Van de Moortel, H. Lipkens, B. Caerts, A. Aerts, L. Giebeler, B. Van Eerdenbrugh, P. Augustijns, G. Van den Mooter, J. Van Humbeeck, J. Vanacken, V. V. Moshchalkov, J. Vermant and J. A. Martens, *Chem. Commun.*, 2008, 49.
- 15 B. Stuyven, G. Vanbutsele, J. Nuyens, J. Vermant and J. A. Martens, *Chem. Eng. Sci.*, 2009, **64**, 1904–1906.
- 16 Z. Shokribousjein, D. R. Galan, C. Michiels, K. Gebruers, H. Verachtert, J. Martens, C. Peeters and G. Derdelinckx, *J. Food Eng.*, 2015, **145**, 10–18.
- 17 The Lubrizol Corporation, Carbopol® 980 NF Polymer, <https://www.lubrizol.com/Health/Pharmaceuticals/Excipients/Carbopol-Polymer-Products/Carbopol-980-NF-Polymer>, accessed 5 December 2019.
- 18 D. Mastropietro, K. Park and H. Omidian, in *Comprehensive Biomaterials II*, ed. P. Ducheyne, Elsevier, Oxford, 2017, vol. 4, pp. 430–444.
- 19 J. Brady, T. Dürig, P. I. Lee and J.-X. Li, in *Developing Solid Oral Dosage Forms*, ed. Y. Qiu, Y. Chen, G. G. Z. Zhang, L. Yu and R. V. Mantri, Academic Press, Boston, 2nd edn, 2016, pp. 181–223.
- 20 I. A. Gutowski, D. Lee, J. R. de Bruyn and B. J. Frisken, *Rheol. Acta*, 2012, **51**, 441–450.
- 21 B. W. Barry and M. C. Meyer, *Int. J. Pharm.*, 1979, **2**, 1–25.
- 22 The Lubrizol Corporation, TDS-237 Neutralizing carbopol and pemulen polymers in aqueous and hydroalcoholic systems, [https://www.lubrizol.com/-/media/Lubrizol/Life-Sciences/Documents/TDS/TDS-237\\_Neutralizing\\_Carbopol\\_Pemulen\\_in\\_Aqueous\\_Hydroalcoholic\\_Systems-PH.pdf](https://www.lubrizol.com/-/media/Lubrizol/Life-Sciences/Documents/TDS/TDS-237_Neutralizing_Carbopol_Pemulen_in_Aqueous_Hydroalcoholic_Systems-PH.pdf), accessed 1 June 2021.
- 23 K. Oka, T. Shibue, N. Sugimura, Y. Watabe, B. Winther-Jensen and H. Nishide, *Sci. Rep.*, 2019, **9**, 223.
- 24 C. Dolce and G. Mériguet, *Colloid Polym. Sci.*, 2017, **295**, 279–287.
- 25 C. Chang, D. D. Muccio and T. St Pierre, *Macromolecules*, 1985, **18**, 2154–2157.
- 26 M. Houllberghs, A. Hoffmann, D. Dom, C. E. A. Kirschhock, F. Taulelle, J. A. Martens and E. Breynaert, *Anal. Chem.*, 2017, **89**, 6940–6943.
- 27 E. Breynaert, M. Houllberghs, S. Radhakrishnan, G. Grübel, F. Taulelle and J. A. Martens, *Chem. Soc. Rev.*, 2020, **49**(9), 2557–2569.

